^{28}Si(p,^{3}He) reaction for spectroscopy of ^{26}Al

K. A. Chipps,[1,2] D. W. Bardayan,[3] K. Y. Chae,[4,5] J. A. Cizewski,[1] R. L. Kozub,[6] C. Matei,[7,*] B. H. Moazen,[5,†] C. D. Nesaraja,[3] P. D. O'Malley,[1] S. D. Pain,[3] W. A. Peters,[1,‡] S. T. Pittman,[5,§] K. T. Schmitt,[5,§] and M. S. Smith[3]

[1]*Department of Physics and Astronomy, Rutgers University, Piscataway, New Jersey 08854, USA*
[2]*Physics Department, Colorado School of Mines, Golden, Colorado 80401, USA*
[3]*Physics Division, Oak Ridge National Laboratory, Oak Ridge, Tennessee 37831, USA*
[4]*Department of Physics, Sungkyunkwan University, Suwon 440-746, Korea*
[5]*Department of Physics and Astronomy, University of Tennessee, Knoxville, Tennessee 37996, USA*
[6]*Department of Physics, Tennessee Technological University, Cookeville, Tennessee 38505, USA*
[7]*Oak Ridge Associated Universities, Oak Ridge, Tennessee 37830, USA*

(Received 19 March 2012; revised manuscript received 18 June 2012; published 30 July 2012)

The ^{28}Si(p,^{3}He)^{26}Al reaction was utilized for the first time to study the levels in ^{26}Al, using a proton beam from the Holifield Radioactive Ion Beam Facility. Five previously unreported states in ^{26}Al are observed and discussed, including Distorted Wave Born Approximation analysis. Proton-decay branching ratios consistent with previous studies and theoretical expectations were found by detecting decay protons from highly excited ^{26}Al states in coincidence with the ^{3}He particles.

DOI: 10.1103/PhysRevC.86.014329 PACS number(s): 25.40.Hs, 26.50.+x, 21.10.−k, 27.30.+t

I. INTRODUCTION

The isotope ^{26}Al is important in many different fields of nuclear physics: in astrophysics for the study of ^{26}Al decay in the galaxy [1–10], as an isotopic chronometer [11,12], and as a benchmark for superallowed Fermi β-decay studies of the weak interaction that probe the Standard Model [13,14], for example. In each case, the specific aspects of the structure of the ^{26}Al nucleus, including excitation energies, spin and parity assignments, branching ratios, spectroscopic factors, and lifetimes, are required for a full understanding of the mechanism being examined. Even as many of these specifics are known [15], there is more to learn about the general structure of ^{26}Al.

Transfer reactions provide a powerful tool to elucidate nuclear structure, and while many studies of ^{26}Al have been made, the (p,^{3}He) transfer reaction has never before been utilized to study ^{26}Al. Similarly, while many proton-capture and proton-scattering measurements have been made in this mass region, coincidence measurements detecting the protons decaying from an excited recoil nucleus (the time-reverse of proton capture) are only very few [16–19]. In addition to studying the ^{28}Si(p, t)^{26}Si*(p) reaction [16], data have also been obtained on ^{26}Al via the ^{28}Si(p,^{3}He) reaction. This paper represents the first spectroscopic application of the ^{28}Si(p,^{3}He) reaction to the study of ^{26}Al levels, as well as the first measurement of proton decay from a transfer reaction to ^{26}Al.

II. EXPERIMENT

A beam of 40-MeV protons, typically between 1 and 2 nA, was delivered from the Holifield Radioactive Ion Beam Facility (HRIBF) 25-MV electrostatic tandem accelerator into a target chamber that contained a 200 μg/cm^2 $^{\text{nat}}$Si (∼92% ^{28}Si) target. The chamber also contained a thick, large-diameter aluminum plate with a collimating aperture just upstream of the target for beam tuning and two arrays of segmented silicon detectors (described below). A diagnostic graphite beam stop was located downstream of the target chamber, with no line-of-sight to the silicon detectors to prevent background signals owing to backscattered beam. The experimental setup is shown in Fig. 1 and is equivalent to that used in the concurrent ^{28}Si(p, t) measurement [16].

Recoiling ^{3}He ions from the ^{28}Si(p,^{3}He) reaction were detected at forward laboratory angles using the highly segmented Silicon Detector Array (SIDAR) [20] covering ∼18° to 50° (∼19°–52° in the center of mass), a configuration similar to that used in Refs. [16,21–23]. For particle identification, SIDAR was arranged into $\Delta E - E$ telescopes with 100-μm energy-loss (ΔE) detectors backed by 1000-μm total-energy (E) detectors. The radial strips of SIDAR allow detection of the ^{3}He particles at several angles simultaneously, with an energy resolution between roughly 80 and 180 keV (FWHM) in the laboratory frame (depending on reaction kinematics). A modified implementation of the Oak Ridge Rutgers University Barrel Array (ORRUBA) [24] was used to cover angles between the edge of SIDAR and ∼90° in the laboratory, as described in more detail in Ref. [16]. While the SIDAR telescopes were used to detect the ^{3}He from the initial ^{28}Si(p,^{3}He)^{26}Al reaction, the ORRUBA detectors were used to detect decay protons from the excited heavy recoil (in this case, ^{26}Al). For this measurement, the decay proton statistics were low and spin parities of the parent levels not well assigned. Thus, proton-coincidence data are only reported as being consistent with existing experimental and theoretical knowledge [25–27] of the ^{25}Mg(p, γ)^{26}Al reaction.

*Current address: EC-JRC Institute for Reference Materials and Measurements, B-2440 Geel, Belgium.
†Current address: USEC, Oak Ridge, Tennessee 37830, USA.
‡Current address: Oak Ridge Associated Universities, Oak Ridge, Tennessee 37830, USA.
§Current address: Physics Division, Oak Ridge National Laboratory, Oak Ridge, Tennessee 37831, USA.

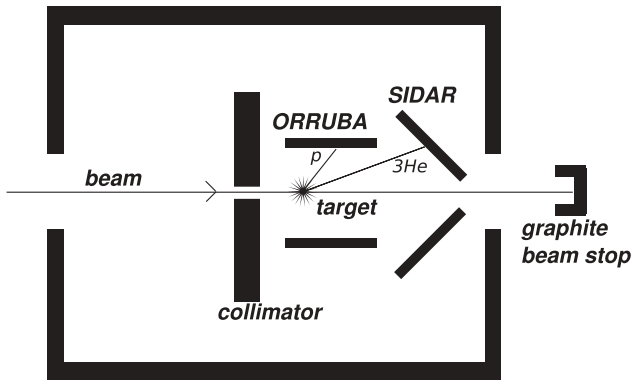

FIG. 1. Experimental setup for the $(p,^3\mathrm{He})$ experiment. Both the Oak Ridge Rutgers University Barrel Array (ORRUBA) and the Silicon Detector Array (SIDAR) are symmetric (in ϕ) about the beam axis. The proton ("p") in the diagram is the decay proton from the ^{26}Al heavy recoil, not the proton beam (which enters from the left).

A. ^{3}He spectra, excitation energies, and angular distributions

By examining a ΔE vs $\Delta E + E$ plot for the SIDAR detectors, the ^{3}He from the desired reaction is easily identified by its energy-loss characteristics, as demonstrated in Fig. 2. Application of software gates allows events in the ^{3}He spectra to be examined without contamination from other reaction products. Contamination of other silicon isotopes in the target is limited to <8% by the target stoichiometry; however, only reactions on ^{28}Si could be identified. Variations in the thickness of each SIDAR detector with respect to the others, small perturbations in the alignment of the target with the detectors between runs, a slight asymmetry in the experimental arrangement, and a beam energy optimized for the (p,t) reaction [16], caused the ^{3}He projectiles from the ground state and isomeric state of ^{26}Al (at around 22 MeV in the laboratory) to punch through both the ΔE and E layers in some of the SIDAR strips. Thus, these two lowest states were not reliably detected in all of the SIDAR detectors. In one SIDAR telescope, however, the asymmetries allowed both the ground state and isomeric state to be consistently observed without

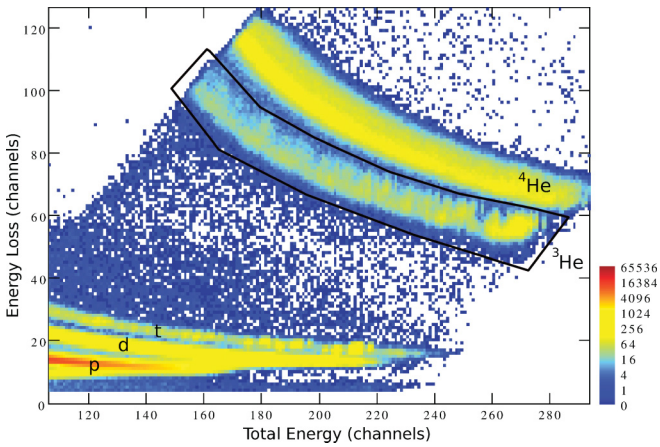

FIG. 2. (Color online) ΔE (vertical) versus $\Delta E + E$ (horizontal) plot from one SIDAR telescope, with the ^{3}He software gate shown in black. Other reaction products are also labeled.

difficulty. To avoid introducing any systematic uncertainties, information from only this one detector telescope was used to extract angular distributions for all of the levels. This had no effect on the calculation of excitation energy for any of the populated levels.

An internal calibration using 16 well-populated, known levels in ^{26}Al [15] was used to locate all other states. The calibration levels ranged from the ground state to an excitation energy of just over 9 MeV, covering the entire range of observed peaks in the ^{3}He spectra. One of the calibration peaks is actually a triplet: $E_x = 2068.86(5) + 2069.47(3) + 2071.64(4)$ keV [15]; however, because the level spacing is significantly smaller than the experimental resolution of this work (roughly 80 keV minimum), it was included in the calibration as $E_x = 2070$ keV. Peaks that were not observed at a majority of detector angles, or which had differing kinematics from the expected reaction, suggesting contaminants, were discounted. In all, 35 peaks were reliably seen in the combined SIDAR spectra. Five of these peaks correspond to levels previously unreported in ^{26}Al. Figure 3 shows the ^{3}He spectrum for two angles in SIDAR. Table I summarizes the excitation energies of the levels populated in this work. The uncertainties in the excitation energies listed in Table I for this work were calculated by treating each of the strips in SIDAR as an independent, simultaneous E_x measurement, using standard analysis methods [28]. While several of the peaks observed could be associated with more than one known level within uncertainty, the nearest known level was adopted save once (see Table I).

Angular distributions were extracted for all of the reliably populated peaks. DWBA calculations were performed for the $(p,^3\mathrm{He})$ reaction with Dwuck4, utilizing the optical model parameters from Ref. [29] and including transfer from the p and sd shells. The validity and robustness of the input parameters for the DWBA calculations were tested against the well-known, strongly populated 0^+ ^{26}Al isomeric state at 228 keV [15]. The 228-keV state displayed a characteristic $\ell = 0$ transition curve for the $(p,^3\mathrm{He})$ reaction, with a maximum peak height of about 3.1×10^7 counts per steradian as shown in Fig. 4, which is compatible with its 0^+ assignment (via coupling to the deuteron's $T = 1$, $S = 0$ configuration). However, most of the previously observed levels [15] displayed relatively flat angular distributions, limiting useful additions to the already known spins and parities. Therefore, only ℓ-transfer values for the states with tentative assignments or previously unobserved levels are reported, and only up to $\ell = 3$ because higher-order transitions are difficult to discern from the data. Angular distributions from the data for previously unknown or tentative levels are compared to DWBA calculations in Fig. 5, presented as counts per steradian to preserve the relative strengths of states to one another (scale is the same as in Fig. 4). The ℓ-transfer results are also presented in Table I.

For the level at 5598 keV, the tentative assignment of $J^\pi = (2,3)^-$ was based on a ^{27}Al$(p,d)^{26}$Al reaction study [30], and is consistent with the measured ℓ transfer from this work. The $(5,6)^+$ assignment for the level at 7921 keV, based on two ^{25}Mg(p,γ) spectroscopy measurements [31,32], is not immediately compatible with the assignment of $\ell = (1,2)$ from this work. However, $\ell \geqslant 4$ could not be ruled out owing to

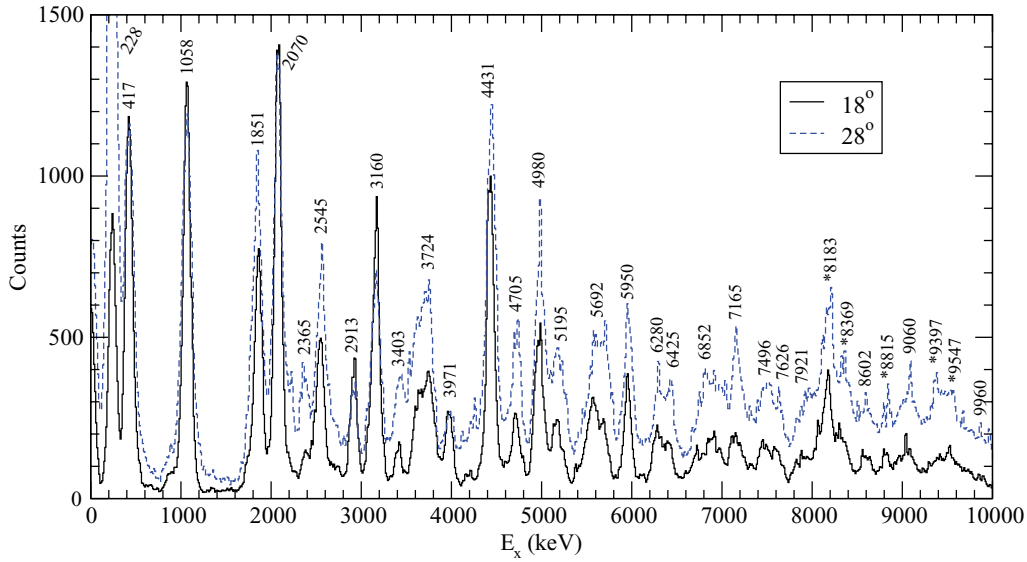

FIG. 3. (Color online) Un-normalized ^{3}He spectrum for SIDAR strips at $\theta_{\rm lab} \sim 18^\circ$ (black solid line) and 28° (blue dashed line). Individual levels are labeled by excitation energy E_x in keV; doublets (see text) are labeled with the average E_x. Previously unreported levels are labeled with an asterisk.

a lack of telling features in the measured angular distribution, such that further constraint on the spin and parity assignment by this work was not possible. The 8602-keV level was best reproduced by $\ell = 1$ transfer, which disagrees with the previous tentative $(5,6)^+$ assignment [32]. Neither transitions with greater than $\ell = 3$ nor multistep reaction processes were considered, however, meaning that a $(5,6)^+$ assignment for this state cannot be completely ruled out.

Because the energy resolution of this measurement was not sufficient to differentiate between very closely adjacent levels, several of the peaks observed are likely doublets. Figure 3 refers to these doublets by the averaged E_x values for the two levels, as determined from the literature, and not by the derived excitation energy from this work. The peak at $E_x = 6417 \pm 19$ corresponds to the two known states $6414.46(10) + 6436.44(11)$ [15]; the angular distribution for this peak does not show a strong $\ell = 0$ shape, indicating the peak is likely an admixture of both the 6414-keV, 0^+ state, and the 6436-keV, 5^+ state (labeled in Fig. 3 as 6425). The peaks observed at $E_x = 7163 \pm 14$, 7489 ± 33, and 7627 ± 20, respectively, correspond to the doublets at $7160.97(9) + 7167.65(6)$, $7495.38(4) + 7497(2)$, and $7622.68(10) + 7627.52(12)$ [15] (labeled in Fig. 3 as 7165, 7496, and 7626). Similarly, the peak at 4978 ± 9 keV is most likely an equal admixture of the known levels at 4952.30 and 5006.66 keV [15] (labeled as 4980), though this would be the widest doublet observed (roughly 50-keV spacing vs ~10-keV spacing). It may be possible that the level observed at $E_x = 6827 \pm 30$ keV is a doublet of the 6817.86(9)- and 6851.50(11)-keV known levels, or potentially associated instead with the 6801.12(4)-, 6801.60(16),- or 6815.74(10)-keV levels (within 1σ). The relatively flat angular distribution for this peak cannot differentiate between the most likely levels. These possible assignments, as well as exclusion of the peak entirely, were applied individually to the calibration to determine the effect. Inclusion of this peak in the calibration and identifying it as only the 6851.50(11)-keV state resulted in an improved fit to the energies of the other known levels, and hence it is the value adopted here. Calculated uncertainties for the derived excitation energies include the effects of this calibration.

B. Candidates for new levels in ^{26}Al

The five previously unreported levels in ^{26}Al, as given in Table I, are $E_x = 8183 \pm 17$, 8369 ± 30, 8815 ± 19, 9397 ± 21, and 9547 ± 22 keV. Owing to the consistent strength, kinematics, and resolution of these peaks, especially when examined in conjunction with known levels in ^{26}Al, they are found to be incompatible with isotopic contamination of the target. For example, for the peaks quoted near 8.1 MeV E_x to be actually attributable to ^{29}Si from the target, they would have to originate from excited levels at nearly 13 MeV in ^{27}Al, with a relative cross section 12 times stronger than the equivalent transition to ^{26}Al; any higher E_x states would be even more difficult to explain as isotopic contaminants. Similarly, their kinematics demonstrates that the peaks are not attributable to environmental contamination of the target (^{12}C, ^{14}N, ^{16}O, etc.).

The observed levels at 8183 ± 17 and 8369 ± 30 keV are several hundred keV away from any known states in ^{26}Al. The level at 8815 ± 19 keV is roughly 100 keV above and below its nearest known neighbors as well. Finally, the two observed states at 9397 ± 21 and 9547 ± 22 keV both fall inside of a ~400-keV gap in known levels. In light of this, we believe it is highly unlikely that any of these newly observed levels correspond to previously known states in ^{26}Al.

C. Decay protons from ^{26}Al

Decay protons from the excited levels in the heavy recoil were detected in six 65-μm-thick nonresistive strip

TABLE I. Excitation energies derived in this work for states populated in ^{28}Si(p,^{3}He)^{26}Al, compared with those of the current ENSDF compilation [15]. If a peak populated in this work potentially corresponds to several known levels (within 1σ), they are listed in parentheses, in order of descending likelihood, after the adopted assignment; only the J^π literature value for the adopted state is given. All states from Ref. [15] are known to sub-keV resolution unless otherwise noted in the table, and therefore are rounded to the nearest keV for ease of comparison. Orbital angular momentum (ℓ) values derived in this work are given for previously unknown or tentative assignments.

E_x (keV)	E_x [15] (keV)	J^π [15]	ℓ
$gs \pm 6$	gs[a]	5^+	
223 ± 10	228[a]	0^+	
424 ± 10	417[a]	3^+	
1061 ± 5	1058[a]	1^+	
1834 ± 9	1851[a]	2^+	
2073 ± 7	2070[a,b]	$4^+, 2^+, 1^+$	
2362 ± 8	2365[a]	3^+	
2552 ± 7	2545[a]	3^+	
2907 ± 4	2913[a]	2^+	
3161 ± 5	3160[a]	2^+	
3417 ± 9	3403[a]	5^+	
3714 ± 15	3724	1^+	
3980 ± 9	3978	0^-	
4439 ± 7	4431[a]	2^-	
4722 ± 9	4705	4^+	
4978 ± 9	4952 + 5007	$3^+, 2^-$	
5196 ± 14	5195[a]	0^+	
5592 ± 31	5598(5585, 5569)	$(2, 3)^-$	(1, 2)
5687 ± 26	5692(5676, 5671)	3^-	
5965 ± 10	5950[a]	1^-	
6290 ± 22	6280(6270)	3^+	
6417 ± 19	6414 + 6436(6399)	$0^+, 5^+$	
6827 ± 30	6852[a] (6818, 6816, 6802, 6801)[e]	2^+	
7163 ± 14	7161 + 7168(7153)	$3^-, 4^-$	
7489 ± 33	7495 + 7497 ± 2(7464)	$3^+, 2^-$	
7627 ± 20	7623 + 7628	$1^+, 5^+$	
7910 ± 29	7921(7891, 7939)	$(5, 6)^+$	(1, 2)
8183 ± 17[c]			(1, 2)
8369 ± 30[c]			2
8616 ± 21	8602	$(5, 6)^+$	1
8815 ± 19[c]			(3)
9060 ± 16	9060[a]	4[d]	(1, 3)
9397 ± 21[c]			(1, 3)
9547 ± 22[c]			(3)
9920 ± 26	9960 ± 10	5^-	

[a]Used as a calibration peak.
[b]This was the only multiplet used as a calibration peak, because the peak was strongly populated and the spacing of the levels is much smaller than the resolution of the experimental setup: 2068.86(5) + 2069.47(3) + 2071.64(4) keV [15].
[c]Assignment from this work (previously unreported).
[d]Parity unknown; see Ref. [15].
[e]The assignment of this state is discussed in more detail in the text.

ORRUBA detectors [24] around the target; this is the same technique used in Ref. [16]. No angular information for the decay protons was available because of the orientation

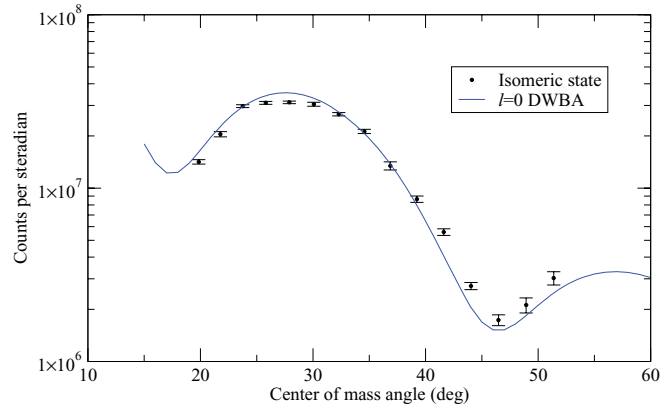

FIG. 4. (Color online) Differential cross section, in counts per steradian, as a function of center-of-mass angle for the isomeric state at 228 keV in ^{26}Al, compared to normalized DWBA calculations for an $\ell = 0$ transition.

of these detectors. The proton separation energy in ^{26}Al is 6306.45 ± 0.05 keV [33]. Several of the known lower-energy resonances in ^{25}Mg(p, γ)^{26}Al were not populated in the ^{3}He spectrum—for instance, the 304-keV resonance at $E_x = 6598$ keV [9], the 254-keV resonance at $E_x = 6551$ keV, or the 198-keV resonance at $E_x = 6496$ keV [4]—and so branching ratios for comparison with such earlier measurements could not be obtained in this work. The levels for which proton branching ratios were measured, as well as the value of the branching ratio B_p, are shown in Fig. 6 and listed in Table II.

The peaks observed in the proton-gated spectra were fit using the known peak-fit parameters from the singles data, unless statistics were such that a fit was unachievable. In this case, a background-subtracted sum within the known width of the singles peak was used. If the statistics were so low as to be unable to estimate background under an individual peak, the raw sum was used, and an estimated background from all angles summed of ∼23%, as determined using a gated area outside the area of interest, was included in the uncertainty. This background resulted in a lower limit to the sensitivity of our setup, which was equivalent to a proton branching ratio of approximately $B_p = 0.2$. Statistical uncertainties were dominated by the low number of proton-gated events, while systematic uncertainties were determined by the "goodness of fit" from both the singles and gated spectra; combined uncertainties are shown in Fig. 6 and given in Table II. Because the proton statistics were so low, occasionally a set of peaks easily resolved in a ^{3}He singles spectrum could not be resolved in the proton-gated spectrum. Therefore, the proton branching ratio of the combined states was calculated by treating the multiple peaks as one single state to improve statistics. This is demonstrated in the horizontal error bars in the bottom panel of Fig. 6.

Most of the higher-energy resonances that were populated in the present study are expected to have predominantly anisotropic decays. Accounting for this unknown anisotropy, which is attributable to unknown, uncertain, or mixed (with unknown ratios) spin and parity assignments of the parent

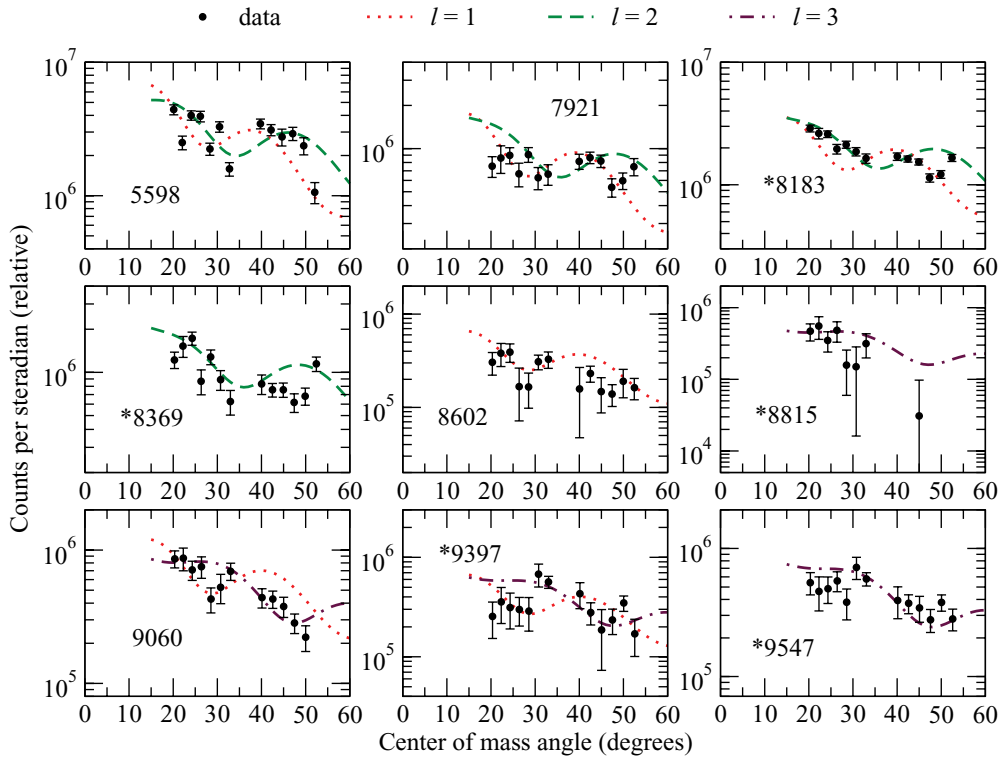

FIG. 5. (Color online) Differential cross sections (in counts per steradian) as a function of center-of-mass angle extracted for the previously unknown levels (labeled with an asterisk) and levels with previously unknown or tentative spin assignments, compared to DWBA calculations. Dotted red line, $\ell = 1$ transfer; dashed green line, $\ell = 2$; dot-dashed purple line, $\ell = 3$.

levels, was not truly feasible. Our previous proton-decay study [16] found corrections to the branching ratios owing to anisotropic decays ($\ell = 1, 2, 3$ vs $\ell = 0$) to be on the order of 5–30%, which is well within the experimental uncertainties in our current data (the magnitude of this effect is similarly seen in, for example, Fig. 9 of Ref. [17]). As such, the values given in Table II and the lower panel of Fig. 6 are calculated assuming purely isotropic decay, and should be taken only as consistent with existing measurements and theory (Refs. [25–27] and the references therein), all of which are already quite well understood. Nearly all of the states have, within uncertainties, a proton branching ratio B_p of approximately 100%, as would be expected for levels falling in between two-particle decay thresholds; the tiny γ widths for these states dominate the resonance strengths [26,27]. The B_p values measured for the previously unreported states at 8183 ± 17, 8369 ± 30, 8815 ± 19, and 9397 ± 21 keV are in agreement with expected values in this excitation energy range, which provides additional support for these states belonging to ^{26}Al.

TABLE II. Proton branching ratios for excited states in ^{26}Al from proton-^{3}He coincidences, assuming isotropic decay. For the states that could not be resolved in the proton-gated spectra, the branching ratio was calculated as though the multiplet was a singlet. Uncertainties are dominated by statistics. See text for further details.

E_x (keV)	B_p^{iso}
6827	0.47 ± 0.24
7163	0.76 ± 0.29
7489 + 7627	0.90 ± 0.65
7910	1.15 ± 0.21
8183	0.70 ± 0.11
8369 + 8616	0.86 ± 0.72
8815	0.78 ± 0.36
9060	0.48 ± 0.15
9397	0.73 ± 0.35

The two levels which do not appear to have branching ratios consistent with one are 6827 ± 30 and 9060 ± 16 keV (both $B_p \sim 50\%$), and there are several reasons why this could be the case. For the 6827 ± 30 keV case, it is possible that this is a real effect if the peak in the proton-gated spectra corresponds to decay of a state with a high angular momentum barrier. Association of this peak with the 4^+ level at 6817.86(9) keV or 6^+ level at 6815.74(10) keV would result in a lower proton branching ratio being observed owing to the increased angular momentum barrier and low energy above the proton separation threshold. However, as previously stated, the energy calibration favors the 6851.50(11) 2^+ level. As the statistics of the proton-gated spectra are worse than the triton-singles spectra, a peak seen in the gated spectra may actually correspond to a different level: For example, while the 6827-keV peak is assigned to the 6852-keV known level

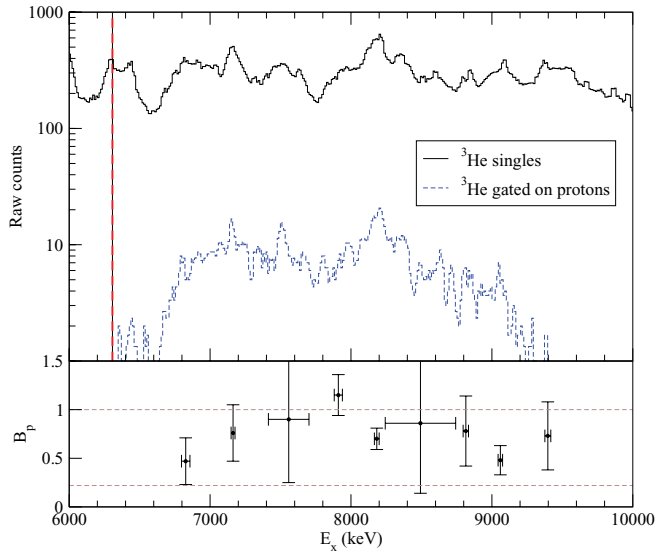

FIG. 6. (Color online) (Top) Number of ^{3}He particles from the $^{28}\mathrm{Si} + p$ reaction observed in the SIDAR strip at $\theta_{\mathrm{lab}} \sim 28^\circ$ as a function of excitation energy (top, solid black line). Peaks are labeled in Fig. 3. The ^{3}He events gated on coincident decay protons (bottom, dashed blue line), uncorrected for geometric efficiency. The red dashed line indicates the proton separation energy in ^{26}Al. (Bottom) Extracted proton branching ratio for the peaks observed in the proton-gated spectra (all angles). Because some of the states seen in the ^{3}He singles spectra could not be resolved in the proton-gated spectra, they are calculated as a combined state, the width of which is indicated by the horizontal error bars. The upper dashed gray line indicates a branching ratio of 100%, and the lower dashed gray line shows the limit of the sensitivity of the experimental setup.

from the triton singles, the peak in the proton-gated spectra may actually correspond to the 6818-keV level, meaning the branching ratio would be incorrectly calculated. Unfortunately, the statistics are such that this potentiality cannot be fully accounted for. It is possible that this is also the case for the 9060 ± 16-keV peak; however, it is not clear precisely why this level otherwise displays such a low branching ratio. There is some evidence from previous measurements in this mass region (see, for instance, Table II in Ref. [17] or Table I in Ref. [18]) of proton branching ratios for levels above the proton separation energy which are not consistent with one, but no additional explanation is given beyond the limits of their statistical uncertainties.

III. CONCLUSION

The isotope ^{26}Al is interesting for many reasons, and thus should be studied with many various techniques. For the first time, the $^{28}\mathrm{Si}(p,^3\mathrm{He})^{26}\mathrm{Al}$ reaction was utilized to study levels in ^{26}Al. This measurement used the same setup for the earlier $^{28}\mathrm{Si}(p,t)^{26}\mathrm{Si}$ study reported in Ref. [16]. Thirty-five levels in ^{26}Al were reliably observed. This included five levels not previously reported in the literature, filling in missing structure information at higher excitation energies in ^{26}Al. DWBA analysis of the new levels, as well as known levels with unknown or tentative spin and parity assignments, yielded previously unmeasured angular distributions and ℓ values for the $^{28}\mathrm{Si}(p,^3\mathrm{He})^{26}\mathrm{Al}^*$ reaction. Coincidence measurements of the decay protons from proton-unbound levels in ^{26}Al added to the small number of previous, similar measurements, demonstrating the continued success of such techniques. Proton branching ratios, while limited by statistics and uncertain J^π information, were found to be generally consistent with expected values. While these specific results do not appear to immediately alter any astrophysical, isochronometer, or β-decay scenarios, they increase the knowledge of the complicated nuclear structure of ^{26}Al and demonstrate that there is more to learn about this important isotope.

ACKNOWLEDGMENTS

We would like to thank the staff of the Holifield Radioactive Ion Beam Facility (HRIBF), and are deeply saddened by its closure. Oak Ridge National Laboratory is managed by UT-Battelle, LLC, for the U.S. Department of Energy (DOE) under Contract No. DE-AC05-00OR22725. This research was supported in part by the National Nuclear Security Administration under the Stewardship Science Academic Alliances program through U.S. DOE Cooperative Agreement No. DE-FG52-08NA28552 with Rutgers University and Oak Ridge Associated Universities. This work was also supported in part by the U.S. DOE under Contracts No. DE-FG02-96ER40955 with Tennessee Technological University and No. DE-FG02-96ER40983 with the University of Tennessee Knoxville and by the National Science Foundation.

[1] R. Diehl *et al.*, Nature (London) **439**, 45 (2006).
[2] L. Buchmann *et al.*, Nucl. Phys. A **415**, 93 (1984).
[3] R. B. Vogelaar, Ph.D. thesis, California Institute of Technology, 1989.
[4] Ch. Iliadis *et al.*, Nucl. Phys. A **512**, 509 (1990).
[5] A. Coc, M.-G. Porquet, and F. Nowacki, Phys. Rev. C **61**, 015801 (1999).
[6] J. Jose, A. Coc, and M. Hernanz, Astrophys. J. **520**, 347 (1999).
[7] G. Lotay, P. J. Woods, D. Seweryniak, M. P. Carpenter, R. V. F. Janssens, and S. Zhu, Phys. Rev. Lett. **102**, 162502 (2009).
[8] W. Wang *et al.*, Astron. Astrophys. **496**, 713 (2009).
[9] B. Limata, F. Strieder, A. Formicola, G. Imbriani, M. Junker, H. W. Becker, D. Bemmerer, A. Best, R. Bonetti, C. Broggini *et al.* (LUNA Collaboration), Phys. Rev. C **82**, 015801 (2010).
[10] S. D. Pain *et al.* (in preparation).
[11] C. Fitoussi, J. Duprat, V. Tatischeff, J. Kiener, F. Naulin, G. Raisbeck, M. Assunção, C. Bourgeois, M. Chabot, A. Coc *et al.*, Phys. Rev. C **78**, 044613 (2008).
[12] M. Bizzarro, J. A. Baker, and H. Haack, Nature (London) **431**, 275 (2004).

[13] P. Finlay, S. Ettenauer, G. C. Ball, J. R. Leslie, C. E. Svensson, C. Andreoiu, R. A. E. Austin, D. Bandyopadhyay, D. S. Cross, G. Demand *et al*., Phys. Rev. Lett. **106**, 032501 (2011).
[14] W. Satuła, J. Dobaczewski, W. Nazarewicz, and M. Rafalski, Phys. Rev. Lett. **106**, 132502 (2011).
[15] P. M. Endt, J. Blachot, R. B. Firestone, and J. Zipkin, Nucl. Phys. A **633**, 1 (1998).
[16] K. A. Chipps, D. W. Bardayan, K. Y. Chae, J. A. Cizewski, R. L. Kozub, J. F. Liang, C. Matei, B. H. Moazen, C. D. Nesaraja, P. D. O'Malley *et al*., Phys. Rev. C **82**, 045803 (2010).
[17] C. M. Deibel, J. A. Clark, R. Lewis, A. Parikh, P. D. Parker, and C. Wrede, Phys. Rev. C **80**, 035806 (2009).
[18] C. Wrede, J. A. Caggiano, J. A. Clark, C. M. Deibel, A. Parikh, and P. D. Parker, Phys. Rev. C **79**, 045803 (2009).
[19] M. Matoš, J. C. Blackmon, L. E. Linhardt, D. W. Bardayan, C. D. Nesaraja, J. A. Clark, C. M. Deibel, P. D. O'Malley, and P. D. Parker, Phys. Rev. C **84**, 055806 (2011).
[20] D. W. Bardayan *et al*., Phys. Rev. C **63**, 065802 (2001).
[21] D. W. Bardayan *et al*., Phys. Rev. C **65**, 032801(R) (2002).
[22] D. W. Bardayan *et al*., Phys. Rev. C **74**, 045804 (2006).
[23] K. Y. Chae, D. W. Bardayan, J. C. Blackmon, K. A. Chipps, R. Hatarik, K. L. Jones, R. L. Kozub, J. F. Liang, C. Matei, B. H. Moazen *et al*., Phys. Rev. C **79**, 055804 (2009).
[24] S. D. Pain *et al*., Nucl. Instrum. Methods B **261**, 1122 (2007).
[25] C. Iliadis, R. Longland, A. E. Champagne, and A. Coc, Nucl. Phys. A **841**, 251 (2010).
[26] NACRE Collaboration, NACRE reaction rate database, http://pntpm3.ulb.ac.be/Nacre/barre_database.htm.
[27] JINA Collaboration, REACLIB reaction rate database, http://groups.nscl.msu.edu/jina/reaclib/db/mg25(p,g)al26/.
[28] P. R. Bevington and D. K. Robinson, *Data Reduction and Error Analysis for the Physical Sciences* (McGraw-Hill, New York, 1992).
[29] K. Y. Chae, D. W. Bardayan, J. C. Blackmon, K. A. Chipps, R. Hatarik, K. L. Jones, R. L. Kozub, J. F. Liang, C. Matei, B. H. Moazen *et al*., Phys. Rev. C **82**, 047302 (2010).
[30] D. L. Show, B. H. Wildenthal, J. A. Nolen, Jr., and E. Kashy, Nuc. Phys. A **263**, 293 (1976).
[31] P. M. Endt, P. de Wit, and C. Alderliesten, Nuc. Phys. A **459**, 61 (1986).
[32] J. Brenneisen, D. Grathwohl, B. Ehrhard, P. M. Endt, S. Fischer, M. Lickert, R. Ott, H. Röpke, J. Schmälzlin, P. Siedle *et al*., Z. Phys. A **354**, 301 (1996).
[33] G. Audi, O. Bersillon, J. Blachot, and A. H. Wapstra, Nucl. Phys. A **729**, 3 (2003).